

Generation of converging strong shock wave formed by microsecond timescale underwater electrical explosion of spherical wire array

O. Antonov, S. Efimov, D. Yanuka, M. Kozlov, V. Tz. Gurovich, and Ya. E. Krasik
 Department of Physics, Technion, Haifa 3200, Israel

(Received 28 February 2013; accepted 18 March 2013; published online 28 March 2013)

A study of generation of converging strong shock wave using microsecond underwater electrical explosion of spherical Cu-wire array is presented. Hydrodynamic simulations coupled with the equation of state for Cu and water, deposited energy, and the magnetic pressure were used to calculate the water parameters in the vicinity of the implosion origin. The results of simulations agree with the shock wave time-of-flight and energy delivered to the water flow and show that in the vicinity (diameter of $\sim 12 \mu\text{m}$) of an implosion one can expect water pressure of $\sim 6 \text{ TPa}$, temperature of $\sim 17 \text{ eV}$, and compression of ~ 8 . © 2013 American Institute of Physics.

[<http://dx.doi.org/10.1063/1.4798827>]

The subject of warm dense matter attracts continuous research attention due to the interesting physical phenomena involved and important technical applications.^{1–3} Several approaches that require stored energy in the range of 10^5 – 10^9 J , such as multi-stage light gas guns,⁴ Z-pinch,⁵ powerful lasers,^{6,7} and intense heavy ion beams,⁸ are used to generate this state of matter,⁹ which is characterized by a pressure $\geq 10^{11} \text{ Pa}$. Recent research^{10,11} showed that underwater electrical explosion of a wire array can be used as an alternative method to generate warm dense matter with $\leq 2 \times 10^{12} \text{ Pa}$, using generators with moderate (several kJ) stored energy. This method is based on the implosion of the converging strong shock wave (SSW) generated by the underwater electrical explosion of either cylindrical or spherical wire arrays. Assuming uniformity of the converging SSW and based on one-dimensional hydrodynamic (1D-HD) simulations, coupled with the equation of state (EOS) of water, the experimentally measured time-of-flight (TOF) of the SSW, and the energy deposited into the water flow, in the case of cylindrical wire arrays explosions^{11–14} the values of pressure, temperature, and density of water in the vicinity of the implosion axis ($r = 2.5 \mu\text{m}$) were estimated as 540 GPa, 3 eV, and 4.2 g/cm^3 , respectively. A significant increase in the parameters of water was achieved in experiments with a sub-microsecond (sub- μs) timescale explosion of a spherical wire array.¹⁵ In this research, the experimental and numerical simulation results indicate that the convergence of the spherical SSW leads to the formation of an extreme state of water in the vicinity ($r = 5 \mu\text{m}$) of the implosion origin that is characterized by pressure, temperature, and density of 2000 GPa, 8 eV, and 7 g/cm^3 , respectively.

In this letter, we present the experimental results of underwater electrical explosion of a spherical wire array using a rather simple microsecond (μs) timescale ($\sim 1.1 \mu\text{s}$) generator¹¹ and a comparison of these results with those obtained in a study that was similar but in which a sub- μs ($\sim 350 \text{ ns}$) timescale high-current generator was used.¹⁵ When a μs timescale generator is used, one can expect that the SSW generated by the explosion of the wire array will propagate for a longer distance under the applied external forces caused by the explosion. The latter could lead to a

larger energy being delivered to the vicinity of the implosion origin, due to the smaller energy losses of the SSW during its implosion.¹⁶

The experimental setup is shown in Fig. 1. A high-current generator¹¹ with stored energy of $\sim 3.6 \text{ kJ}$ generates a current pulse with an amplitude of $\sim 300 \text{ kA}$ and rise time of $\sim 1.1 \mu\text{s}$, which is applied to the spherical Cu wire array.¹⁵ The explosion of the wires is accompanied by the generation of shock waves whose overlapping results in the formation of a converging SSW. In the experiments, various diameters (20 mm, 30 mm, 40 mm) of the wire array and various numbers (20–40) and diameters (100–160 μm) of the Cu wires were tested to achieve aperiodic electrical discharge when almost all (up to 80%) of the initially stored energy is deposited to the wire array within $\sim 600 \text{ ns}$.

The discharged voltage and current, measured by the voltage divider and Rogowski coil, respectively, were used to calculate the energy deposition rate, $P = I \times V_r$, into the exploding wires (see Fig. 2). As in the experiments described in Ref. 15, to measure the TOF of the converging SSW, a 1-mm in diameter optical fiber was placed along the equatorial diameter of the spherical wire array. This fiber was destroyed by the converging SSW when the latter approached the vicinity of the implosion origin. The damage to the fiber occurred exactly in the center of the sphere.¹⁵ The destruction of the fiber results in a strong light emission appearing, which was measured by a R7400U-04 photomultiplier tube (see Fig. 3). Depending on the wire array diameter, the time of the SSW's arrival at the origin of the implosion was different. Namely, when 20-mm, 30-mm, and 40-mm diameter arrays were used, these times were $4 \pm 0.2 \mu\text{s}$, $6 \pm 0.2 \mu\text{s}$, and $9.3 \pm 0.2 \mu\text{s}$ with respect to the beginning ($t = 0$) of the discharge current. For each wire array diameter, at least six explosions were conducted to estimate the error bars of the TOF data. The generation of the SSW starts at $t \approx 1 \mu\text{s}$ when the wire explosion begins, with a corresponding fast radial expansion of the wires.

Here let us note that the obtained data showed a smaller TOF (by several hundreds of ns with respect to time when the maximum power is obtained) of the SSW than that obtained in sub- μs experiments¹⁵ carried out using identical

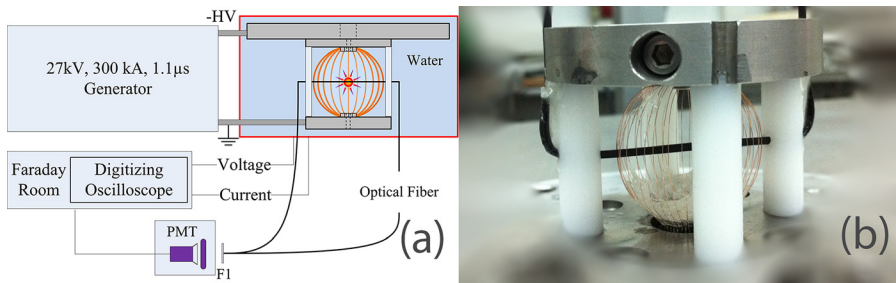


FIG. 1. (a) Experimental setup. F1 is the optical filter. (b) External view of the wire array of 30 mm in diameter and composed of 40 Cu wires each of 114 μm in diameter.

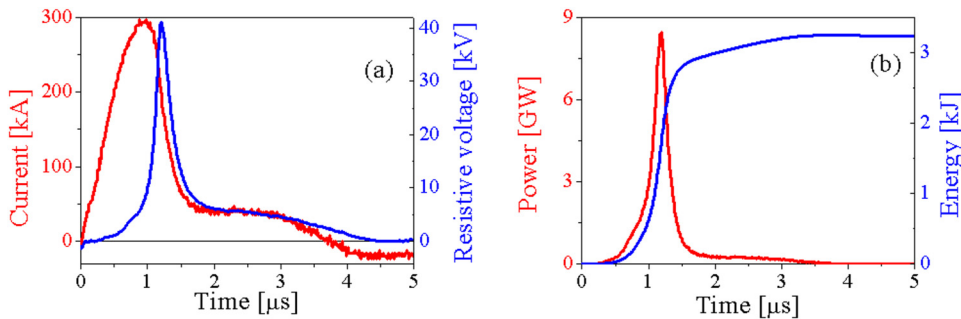


FIG. 2. Waveforms of (a) discharged current and the resistive voltage and (b) deposited power and energy. The wire array, consisting of 40 Cu wires, each 100 μm in diameter, was 40 mm in diameter.

wire arrays, but almost two times more initially stored energy. The latter strongly indicates a faster SSW propagation and, respectively, a larger pressure, density, and temperature, which one might expect in the vicinity of the implosion origin.

Our first attempts to calculate the parameters of the water in the vicinity of the origin, assuming uniformity of the converging SSW and using simplified 1D HD simulation¹⁵ coupled with EOS for water, failed. This happened because these calculations required the energy deposited into the wire array to be ~ 4 times larger than the initially stored energy in order to satisfy the experimentally measured TOF data. Thus, to explain the fast TOF data and to avoid contradiction with the deposited energy, it was decided to consider the acceleration of the wires and, respectively, the water layer adjusting to wires, by taking into account the self-magnetic field gradient of the discharge current. Indeed, in the case of a μs timescale current pulse, this force could be non-negligible as compared with that in a sub- μs timescale wire array explosion. Therefore, modifications were made for numerical simulations which should consider this effect.

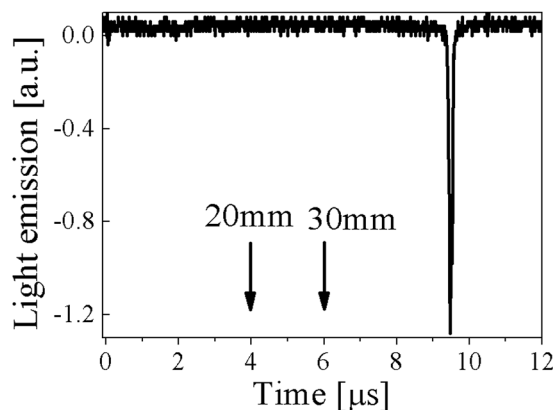


FIG. 3. Typical waveform of light-emission from the optical fiber. The wire array, consisting of 40 Cu wires, each 100 μm in diameter, was 40 mm in diameter. Here $t = 0$ is the time of the beginning of the discharge current.

In order to calculate the parameters of the water in the vicinity of the implosion, one can use a simple piston model, described in Ref. 13, where the total energy deposited into the water flow was supposed to be equal to the work of the piston. The temporal evolution of the piston's velocity is described as $v = \alpha(t - t_0)(t - t_f)$, where t_0 is the time of the beginning of the wire explosion, t_f is the time when $\sim 70\%$ of the initially stored energy was delivered to the exploding wires, and α is the parameter that was adjusted to achieve correspondence with the TOF data and the energy delivered to the water flow by the piston, which should be $\leq 12\%$ of the total energy delivered to the exploding wires.¹⁷ In the case of the magnetic pressure, transferring momentum to the piston, the time t_0 becomes significantly smaller because magnetic force acts on the wires also prior to the beginning of wires explosion. The smaller is the radius of the wire array, the larger is the magnetic pressure. Therefore, for a smaller wire array one has to decrease the value of t_0 in order to obtain matching between the magnetic energy deposition and the work done by the piston. Simulations showed that the typical value of the efficiency of the magnetic energy transfer to the water flow is $\leq 40\%$ of the total ($\omega_m \approx 350 \text{ J}$) magnetic energy. This relatively poor efficiency can be related to the finite transparency of the wire array and friction, which were not taken into account in these simplified simulations. Using this model, water parameters in the vicinity of the implosion origin were calculated for different diameters of the wire arrays (see Table I). One can see that the smaller is the wire array diameter, the larger are the values of pressure, temperature, and water compression. Namely, in the case of a 20-mm diameter wire array one can expect a water volume with a diameter of $\sim 12 \mu\text{m}$ with pressure, temperature, and compression up to 6.6 TPa, 17 eV, and 9, respectively, when the SSW is reflected from the origin of its implosion.

In addition, other 1D HD simulations¹⁵ were carried out in order to draw a comparison with the results of the piston model. In these simulations, the SSW generation and propagation velocity were governed not by a converging piston with a defined

TABLE I. P_1 , T_1 , and δ_1 are the pressure, temperature, and compression factor of water, respectively, when the SSW front approaches a radius of $6 \mu\text{m}$. P_m , T_m , and δ_m are the pressure, temperature, and compression, respectively, at the moment when the converging SSW is reflected from the origin and approaches a radius of $6 \mu\text{m}$.

| Array diameter [mm] | Number of wires | Dia. of wire [μm] | P_1 [TPa] | T_1 [eV] | δ_1 | P_m [TPa] | T_m [eV] | δ_m |
|---------------------|-----------------|--------------------------------|---------------|----------------|---------------|---------------|----------------|-----------------|
| 40 | 32–40 | 100 | 1.1 ± 0.1 | 7.2 ± 1 | 4.7 ± 0.1 | 3.8 ± 0.3 | 11 ± 1.4 | 7.45 ± 0.25 |
| 30 | 36–40 | 100–130 | 2 ± 0.2 | 12.5 ± 1 | 4.9 ± 0.1 | 5.3 ± 0.2 | 16 ± 1.6 | 8.5 ± 0.2 |
| 20 | 30–40 | 100–130 | 3.5 ± 0.3 | 18.5 ± 1.3 | 6 ± 0.1 | 6 ± 0.6 | 15.6 ± 1.3 | 8.75 ± 0.15 |

time-dependent velocity but by the self-consistent expansion of a 1D cylindrical “Cu layer” having the same total mass as the exploded wires into which the electrical energy was deposited. The entire simulated volume was divided into the exploding “Cu layer” and water layers inside and outside the “Cu layer.” The deposition of the energy into the “Cu layer” was calculated using the obtained resistive voltage and discharge current. These 1D HD simulations were coupled with the SESAME database of EOS¹⁸ for Cu and water and were modified to take into account the energy delivered to this “Cu layer” by the magnetic field pressure. Parameters of the water in the vicinity of the implosion origin obtained using these simulations were in satisfactory agreement ($10\% \pm 2\%$) with the results of the piston model. Let us note that the results of both the models were checked for the energy being transferred to the water flow to be $12\% \pm 1\%$ of the energy deposited into the exploding wire.¹⁷

In Ref. 15, a similar research study is reported using a sub- μs timescale generator with almost twice the stored energy of $\sim 6 \text{ kJ}$. In this publication, the water parameters (pressure, temperature, and density) were presented for a sphere with a radius of $3 \mu\text{m}$. To compare these results with the results of the present study, one can calculate the pressure using self-similarity analysis¹⁰ for the spherical case $P(r_c) \propto E_w r_0^{-1.67} r_c^{-1.33}$. For example, in Ref. 15, for a 30 mm diameter wire array, the pressure reported was 4 TPa inside a sphere with radius of $3 \mu\text{m}$; thus, $P(r_c = 6 \mu\text{m}) = 1.6 [\text{TPa}]$, which is noticeably smaller than the calculated pressure in the present experiment ($2.1 \pm 0.2 \text{ TPa}$), in spite of the larger energy deposited into the wire array. In addition, in Fig. 4 one can see the time-dependent radial position of the pressure of $\geq 100 \text{ GPa}$ at the SSW front for the present experiments and those described in Ref. 15 in the case of a 30-mm

diameter wire array explosion. One can see that in μs time-scale experiments the duration and radius where this pressure exists in water increases ~ 1.5 times.

Thus, the results of the present study confirmed one of the main conclusions of simulations.¹⁶ Namely, despite a smaller energy being deposited into the wire array, one can obtain larger pressure in the vicinity of SSW implosion if a proper adjustment between the SSW TOF and energy deposition rate is achieved. To conclude, the μs timescale underwater electrical explosion of a spherical wire array using a generator with stored energy of only $\sim 3.6 \text{ kJ}$ showed parameters of the extreme state of water in the vicinity of the implosion origin that were superior to those obtained in sub- μs time scale experiments, due to the additional input of magnetic gradient force. Using 1D HD numerical calculation, the extreme state of water in a sphere with diameter of $\sim 12 \mu\text{m}$ can be characterized by pressure, temperature, and compression of $\leq 6 \text{ TPa}$, $\leq 17 \text{ eV}$, and ≤ 8 , respectively.

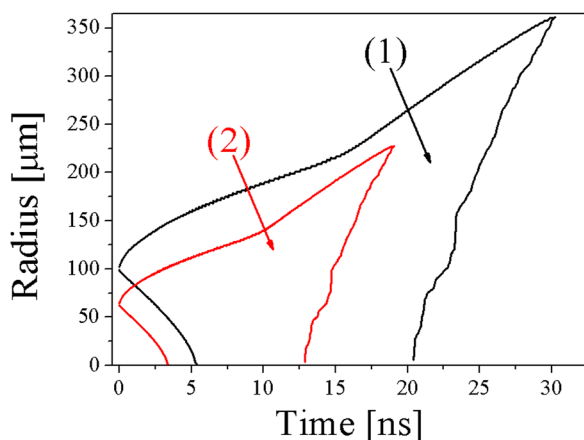


FIG. 4. Time evolution of the radial position of a 100 GPa pressure in water generated by (1) μs timescale and (2) sub- μs timescale underwater electrical explosions of a 30-mm Cu wire array, with respect to the first moment when the pressure at the front of the SSW becomes $\geq 100 \text{ GPa}$.

¹E. A. Martin, *J. Appl. Phys.* **31**, 255 (1960).

²A. V. Luchinskii, *Electrical Explosion of Wires* (Nauka, Moscow, 1989).

³S. V. Lebedev and A. I. Savvatimski, *Sov. Phys. Usp.* **27**, 749 (1984).

⁴A. C. Mitchel and W. J. Nellis, *Rev. Sci. Instrum.* **52**, 347 (1981).

⁵R. B. Spielman, C. Deeney, G. A. Chandler, M. R. Douglas, D. L. Fehl, M. K. Matzen, D. H. McDaniel, J. T. Nash, J. L. Porter, T. W. L. Sanford, J. F. Seaman, W. A. Stygar, K. W. Struve, S. P. Breeze, J. S. McGurn, J. A. Torres, D. M. Zagar, T. L. Gilliland, D. O. Jobe, J. L. McKenney, R. C. Mock, M. Vargas, T. Wagone, and D. L. Peterson, *Phys. Plasmas* **5**, 2105 (1998).

⁶P. M. Celliers, G. W. Collins, D. G. Hicks, M. Koenig, E. Henry, A. Benuzzi-Mounaix, D. Batani, D. K. Bradley, L. B. Da Silva, R. J. Wallace, S. J. Moon, J. H. Eggert, K. K. M. Lee, L. R. Benedetti, R. Jeanloz, I. Maschiet, N. Dague, B. Marchet, M. R. Le Gloahac, Ch. Reverdin, J. Pasley, O. Willi, D. Neely, and C. Danson, *Phys. Plasmas* **11**, L41 (2004).

⁷K. Kolacek, V. Prukner, J. Schmidt, O. Frolov, and J. Straus, *Laser Part. Beams* **28**, 61 (2010).

⁸N. A. Tahir, Th. Stöhlker, A. Shutov, I. V. Lonosov, V. E. Fortov, M. French, N. Nettelmann, R. Redmer, A. R. Piriz, C. Deutch, Y. Zhao, H. Xu, G. Xiao, and W. Zhan, *New J. Phys.* **12**, 073022 (2010).

⁹T. Sasaki, Y. Yano, M. Nakajima, T. Kawamura, and K. Horioka, *Laser Part. Beams* **24**, 371 (2006).

¹⁰A. Grinenko, V. Tz. Gurovich, and Ya. E. Krasik, *Phys. Plasmas* **14**, 012701 (2007).

¹¹S. Efimov, A. Fedotov, S. Gleizer, V. Tz. Gurovich, G. Bazalitski, and Ya. E. Krasik, *Phys. Plasmas* **15**, 112703 (2008).

¹²A. Fedotov-Gefen, S. Efimov, L. Gilburd, S. Gleizer, G. Bazalitskiy, V. Tz. Gurovich, and Ya. E. Krasik, *Appl. Phys. Lett.* **96**, 221502 (2010).

¹³A. Fedotov-Gefen, S. Efimov, L. Gilburd, G. Bazalitski, V. Tz. Gurovich, and Ya. E. Krasik, *Phys. Plasmas* **18**, 062701 (2011).

¹⁴L. Gilburd, S. Efimov, A. Fedotov-Gefen, V. Tz. Gurovich, G. Bazalitskiy, O. Antonov, and Ya. E. Krasik, *Laser Part. Beams* **30**, 215 (2012).

¹⁵O. Antonov, L. Gilburd, S. Efimov, G. Bazalitski, V. Tz. Gurovich, and Ya. E. Krasik, *Phys. Plasmas* **19**, 102702 (2012).

¹⁶G. Bazalitski, V. Ts. Gurovich, A. Fedotov-Gefen, S. Efimov, and Ya. E. Krasik, *Shock Waves* **21**, 0321 (2011).

¹⁷S. P. Lyon and J. D. Johnson, Report No. LA-UR-92-3407, SESAME: The Los Alamos National Laboratory, 1992.

¹⁸S. Efimov, V. Tz. Gurovich, G. Bazalitski, A. Fedotov, and Ya. E. Krasik, *J. Appl. Phys.* **106**, 073308 (2009).